Iron-Sulfur Clusters: Nature's Modular, Multipurpose Structures

Helmut Beinert, Richard H. Holm, Eckard Münck

Iron-sulfur proteins are found in all life forms. Most frequently, they contain Fe_2S_2, Fe_3S_4, and Fe_4S_4 clusters. These modular clusters undergo oxidation-reduction reactions, may be inserted or removed from proteins, can influence protein structure by preferential side chain ligation, and can be interconverted. In addition to their electron transfer function, iron-sulfur clusters act as catalytic centers and sensors of iron and oxygen. Their most common oxidation states are paramagnetic and present significant challenges for understanding the magnetic properties of mixed valence systems. Iron-sulfur clusters now rank with such biological prosthetic groups as hemes and flavins in pervasive occurrence and multiplicity of function.

Iron-sulfur clusters are common to the most ancient components of living matter, yet it was not until around 1960 that—in studies on photosynthetic organisms (*1*), nitrogen-fixing bacteria (*2*), and submitochondrial fractions of mammalian origin (*3*)—signs were gleaned that there existed thus far unknown proteins that were involved in biological oxidoreductive functions. These proteins were soon found to contain iron and to represent a single family of iron proteins (*4*). Those in plants and microorganisms were of low molecular weight and were water-soluble, whereas those from mammals were membrane-bound. By the mid-1960s, these proteins were shown to contain complexes of iron and cysteinate (Cys) sulfur atoms and to incorporate inorganic or "acid-labile" sulfide in the form of two- and four-iron clusters (*4*). Since then, our knowledge of iron-sulfur proteins has grown exponentially (*5–7*). They are ubiquitous in living matter and contain sites with one to eight iron atoms, sometimes with multiple occurrence of the smaller clusters in the same protein molecule.

In the 1970s, it was demonstrated that iron-sulfur species of nuclearities 1, 2, and 4 could be synthesized (*6, 8*). As more detailed geometric and electronic structural data were gained, it became evident that these synthetic complexes are accurate analogs of the protein-bound sites. This result immediately proved that protein structure is unnecessary for the sites' existence. Deviations from the intrinsic properties of these molecules reflect the influence of protein structure and environment, which cannot be readily assessed in any other way. Summarized in Fig. 1 are synthetic routes to analog molecules starting with an Fe(II) source, which is easily converted to mononuclear **1** and the cage complex **2** by reactions 1 and 2, respectively. Binuclear **3** and linear trinuclear **4** are accessible through redox reactions 3 and 4 of precursor **1**. In the similar reaction 5, **2** is converted to the cubane cluster **5a**. The last member of the set, cuboidal cluster **6**, is considerably less stable; its synthesis has recently been achieved (*9*). Mononuclear site **1** and clusters **3**, **5**, and **6** are common constituents of proteins, with **3** and **5a** being especially pervasive. The structures of protein sites **1**, **3**, **5**, and **6** have been established by crystallography (*7*). The mechanisms of cluster biosynthesis are unknown. However, proteins containing clusters **3** and **5a** are readily formed in high yield in vitro by apoprotein reconstitution reactions 18 and 8, respectively, which were first demonstrated in the 1960s. Native clusters of even higher nuclearity can be constructed by bridging individual cuboidal modules (Fe_4S_3, $MoFe_3S_3$) with sulfide and thiolate, as in the P cluster (Fe_8S_7) and cofactor cluster ($MoFe_7S_9$) of nitrogenase (*10*), with the indicated core compositions (Fig. 2). These are the largest known native iron-sulfur clusters. Additional complex sites have evolved in which an Fe_4S_4 cluster is bridged by a Cys sulfur atom to a heme group in sulfite reductase (*11*) or by an unknown atom to a nickel center in the two distinct clusters of carbon monoxide dehydrogenase (*12*).

Cluster Conversions

Iron-sulfur clusters have a remarkable facility for conversion and interconversion in both the free and protein-bound conditions, supporting the concept that they are modular structures. They also undergo ligand exchange reactions and oxidative degradation, both of which are biologically significant.

Before we consider the numerous uses for iron-sulfur proteins that nature has evolved, we draw attention to their remarkable structural versatility, which forms the basis for their various functions. Initially, the impression was gained that the clusters in proteins, when placed in aqueous solution in the presence of dioxygen, would readily decay when removed from the protein scaffolding supporting them. To an extent, this impression was reinforced by synthetic clusters, which are usually manipulated in aprotic anaerobic solvents. The term "cofactor," in the sense that it was used for organic cofactors, did not seem appropriate. However, when methods were designed to "extrude" protein-bound clusters from (reactions 9 and 19) or transfer them between different (apo)proteins in the presence of mild denaturants and carrier thiols (*13*), the impression of the fragility of clusters had to be revised. Although these are sensitive molecules, especially in the presence of acids and oxidants, they are more robust, more cofactor-like, than originally thought.

The next revision of thought necessary for an eventually full appreciation of the chemical properties of clusters followed from observations of the conversion of one structure to another, the earliest example of which was $2[Fe_2S_2]^{1+} \rightarrow [Fe_4S_4]^{2+} + [Fe_4S_4]^{2+}$ (reaction 7) in synthetic complexes. (In describing clusters and their reactions, it is convenient to do so in terms of the cluster core, such that oxidation levels are immediately apparent.) The next instances were encountered with *Desulfovibrio gigas* ferredoxin II and the enzyme aconitase, in which facile interconversion between the cubane $[Fe_4S_4]^{2+}$ and cuboidal $[Fe_3S_4]^{1+}$ structures occurs (reaction 12) (*14, 15*). Aconitase is inactive in the Fe_3S_4 state (*16*). The spontaneous cluster reconstruction **6** → **5b** is the self-activation of aconitase, restoring the catalytic center with one substitutionally labile iron subsite where substrate binds. Even more remarkable reorganization of protein-bound clusters followed and can be categorized under the term "Cys ligand swapping" (*17*). A striking example was reported, again with aconitase: When the inactive $[Fe_3S_4]^{1+}$ form of the enzyme was exposed to pH > 9 or treated with urea, a purple chromophore was generated (*18*). Spectroscopic studies and property compar-

H. Beinert is in the Institute for Enzyme Research and the Department of Biochemistry, University of Wisconsin, Madison, WI 53705, USA. R. H. Holm is in the Department of Chemistry and Chemical Biology, Harvard University, Cambridge, MA 02138, USA. E. Münck is in the Department of Chemistry, Carnegie Mellon University, Pittsburgh, PA 15213, USA.

ison with synthetic $[Fe_3S_4(SR)_4]^{3-}$ clusters of known structure (*19*) demonstrated the conversion from cuboidal **6** to linear **4** (reaction 11), now with four Cys ligands in complex **4** instead of three. One of the original Cys ligands was released, and two new Cys ligands were recruited from a more distant α helix, as far as 14 and 17 Å away. Simultaneously, a significant amount of Fe_2S_2 cluster **3** was formed. When the pH was lowered and an iron salt and thiol were added, >60% of the $[Fe_4S_4]^{2+}$ cluster **5b** could be reconstituted from the linear $[Fe_3S_4]^{1+}$ form (reaction 10), and the corresponding enzymatic activity was regained. The conversion of linear **4** to the cubane cluster **5** by reaction with Fe^{2+} and a reductant occurs readily in synthetic systems (*19*).

In addition to being converted to linear **4** and the cubane **5,** cuboidal **6** exhibits another type of reactivity in both proteins (*20, 21*) and synthetic systems (*22*). Upon reduction to the $[Fe_3S_4]^0$ oxidation state (reaction 13), or to the $[Fe_3S_4]^{1-}$ state when associated with metal ions, these species tightly bind metal ions to form heterometal MFe_3S_4 cubane clusters **7** (reaction 14). Reduction below the $[Fe_3S_4]^{1+}$ state is necessary to render the sulfur atoms that bridge two iron atoms (μ_2-S) sufficiently nucleophilic to bind metal ions. Alternatively, in synthetic systems, **4** reacts with reduced metals [Co(I), Ni(0)] to afford **7** directly. In these cases, the reductive rearrangement (reaction 20) proceeds by an inner-sphere pathway in which electron transfer between the metal and the cluster causes the latter to fold and bind the oxidized metal [Co(II), Ni(II)]. Metal ion incorporation (reaction 14) emphasizes the modular nature of cuboidal Fe_3S_4 species, which function as tridentate cluster ligands. Given the widespread occurrence of cuboidal clusters in proteins, one might expect to find native MFe_3S_4 clusters formed under reducing conditions. Reaction 14 is the heterometal version of reconstitution reaction 12. The scope of heterometal cubanes has been substantially widened by Coucouvanis and co-workers (*23*), who have simulated reductions of nitrogenase substrates using such cubanes and have synthesized bridged double cubanes.

As early as 1984 it was reported (*24*), and later independently confirmed (*25*), that the $[Fe_4S_4]^{2+}$ form **5a** of the iron protein of nitrogenase, when exposed to a chelator in the presence of Mg adenosine triphosphate, was converted in significant yield to an Fe_2S_2 cluster **3** (reaction 16). This is the most direct conversion of the two cluster types in proteins, the formation of **3** in aconitase proceeding through trinuclear **6** under denaturing conditions. More recently, however, an almost quantitative conversion of **5a** to **3** was observed on exposure of the FNR (fumarate nitrate reduction) protein of *Escherichia coli* to dioxygen (*26*). This protein is a transcriptional activator that controls numerous genes required for the synthesis of components of the anaerobic respiratory pathways of *E. coli* where substrates such as fumarate or nitrate serve as oxidants instead of dioxygen. When isolated aerobically, FNR is inactive and occurs as a 30-kD monomer. The active protein is dimeric and contains two $[Fe_4S_4]^{2+}$ clusters per dimer (*27*). On exposure to dioxygen, these are readily converted to $[Fe_2S_2]^{2+}$ clusters, which are stable but do not sustain FNR activity. This work demonstrates that reaction 17 can occur with a pure protein and without any reagents that are not found naturally.

Ligand Swapping Without Cluster Conversion

Observations of similarly unexpected ligand swapping have been reported for other proteins in which the number of Cys residues exceeds that required for ligand binding to clusters. *Azotobacter vinelandii* ferredoxin contains 107 residues, of which eight are Cys; seven of these bind the two clusters present, cuboidal Fe_3S_4 and cubane Fe_4S_4. Site-directed mutagenesis of Cys^{20}, a ligand to the Fe_4S_4 cluster, to Ala causes Cys^{24}, a

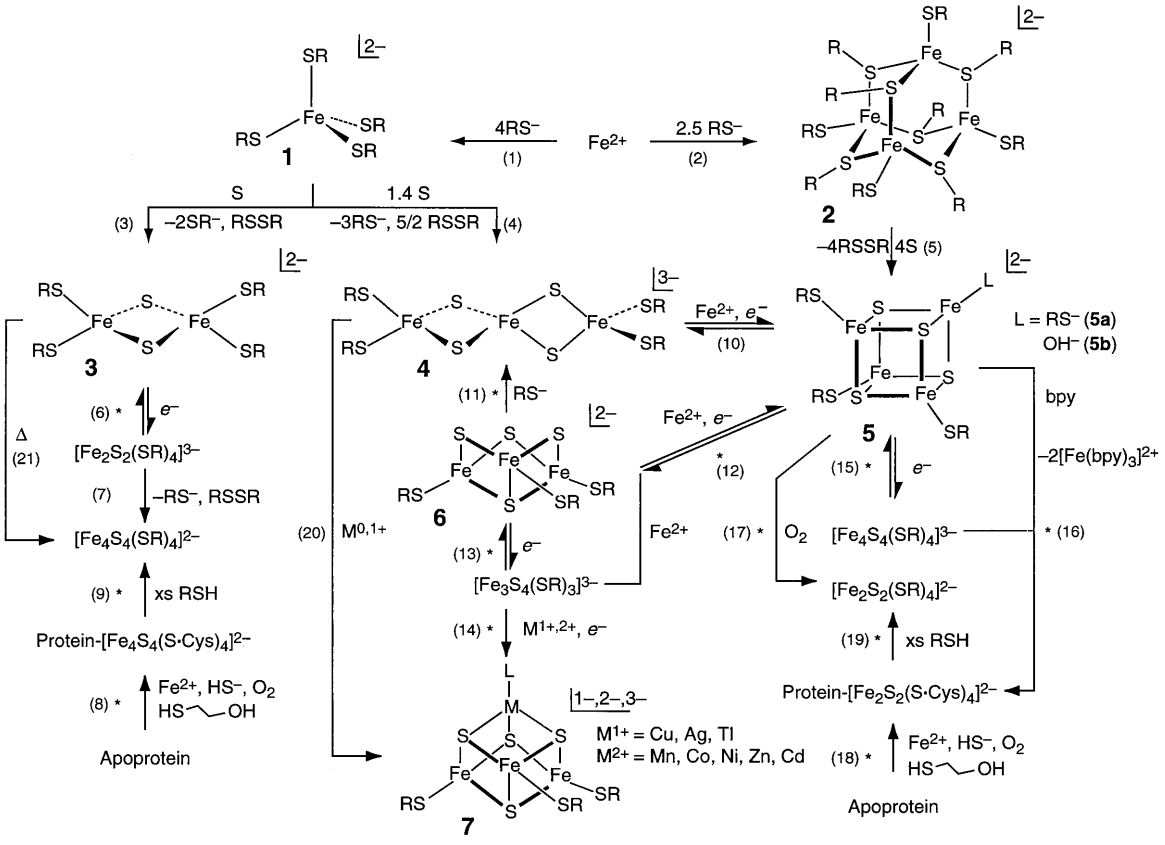

Fig. 1. Reaction scheme of iron-sulfur clusters **3** through **7** showing their synthesis in vitro from Fe (II) complexes **1** and **2** and elemental sulfur, cluster conversions and interconversions, and associated reactions (labeled 1 to 21 by numbers in parentheses). The ligands RS^- are alkyl or aryl thiolates in synthetic clusters and cysteinyl residues in proteins; overall cluster charges (core plus ligands) are indicated. All known protein-bound clusters with nuclearity four or less and their well-documented transformations (*) are included. (bpy = 2,2′-bipyridyl, L = ligand, xs = excess, Δ = heat).

free residue in the native protein, to bind to this cluster. When Cys^{20} is mutated to Ser, the cluster rejects oxygen ligation in favor of Cys^{24} (*28*). The ferredoxin from *Clostridium pasteurianum* (*Cp*)—containing one Fe_2S_2 cluster and 102 residues with five Cys residues at positions 11, 14, 24, 56, and 60—is another interesting case (*17*). Residues 11, 56, and 60 were unambiguously shown to be cluster ligands by replacement through recombinant DNA techniques, whereas no decisive answer could be obtained for residues 14 and 24. It turns out that either Cys, although they are nine residues apart, can serve as a ligand because of its presence in a structurally flexible loop. A subunit of the NADH (reduced nicotinamide adenine dinucleotide) quinone oxidoreductase of *Paracoccus denitrificans* (*Pd*), although showing very little sequence homology, has a spacing of Cys residues equivalent to $Cys^{11,56,60}$ of *Cp* ferredoxin. The fourth Cys ligand to the Fe_2S_2 cluster of the *Pd* protein corresponds to position 16 in the *Cp* protein. When Leu^{16} of the latter protein was substituted with Cys, and Cys^{14} and Cys^{24} were substituted with Ala, Cys^{16} became a cluster ligand. It was also found that a stretch of up to 14 residues (19 to 32) could be deleted with no deleterious effect on protein stability or modification of spectroscopic properties (*17*). In all of these cases, the avidity of cluster iron atoms for Cys coordination drives the rearrangement of protein structure.

Core Transformations

Sulfide atoms in the cores of free and protein-bound clusters **3**, **5**, and **6** are subject to exchange with external sulfide in the absence of thiols or denaturing agents. For example, after addition of ^{35}S (sulfide), the isotope is found in the Fe_3S_4 core of aconitase within minutes, and three of the four sulfides—presumably μ_2-S atoms, which bridge only two iron atoms—exchange completely in 1 to 2 hours. The fourth sulfide exchanges more slowly, within 5 to 10 hours (*29*). Because sulfide is a reductant, the initial $[Fe_3S_4]^{1+}$ state may be reduced to $[Fe_3S_4]^0$, with which the actual exchange proceeds. Sulfide exchange is slower in the active (Fe_4S_4) form of aconitase, where all sulfides are of the μ_3-S type, and substrate inhibits exchange. In the presence of a large excess of sulfide, the cluster disintegrates. Synthetic clusters **3** and **5a** readily incorporate selenide into the core when exposed to a soluble source such as Li_2Se in tetrahydrofuran. Further, when the cluster pairs $[Fe_4S_4(SR)_4]^z$/$[Fe_4Se_4(SR)_4]^z$ with $z = 2-$ or $3-$ are placed in acetonitrile solution, the mixed ligand clusters $[Fe_4S_{4-n}Se_n(SR)_4]^z$ ($n = 0$ to 4) are formed in approximately statistical amounts (*30*). In the $z = 3-$ system, all species are observable at room temperature after several hours, but the $z = 2-$ clusters require heating at ~50°C for extended periods to approach equilibrium. The mechanism of intercluster chalcogenide atom exchange, in particular, is decidedly unclear. The much more facile exchange between reduced cores may be associated with their somewhat longer (0.05 to 0.1 Å) and weaker Fe–S and Fe–Se bonds. In the context of these reactions, the cores could be described as "quasi-permeable" to sulfide. We also note that, whereas the core dimensions of $[Fe_2S_2]^{2+}$ rhombs and tetragonally distorted $[Fe_4S_4]^{2+}$ cubanes vary little with extrinsic factors, the geometries of $[Fe_4S_4]^{1+}$ cores take on various distortions from idealized cubic symmetry that cannot yet be correlated with extrinsic features or with any intrinsic property such as spin state (*31*). In this sense, the reduced $[Fe_4S_4]^{1+}$ cores have a structural "plasticity" that may be related to their enhanced reactivity toward chalcogenide exchange.

Functions Beyond Electron Transfer

Given the structural and reactivity properties of iron-sulfur clusters, it is no surprise that in the course of evolution, multiple uses of these clusters have developed in addition to that first recognized, namely, electron transfer (*4*, *32*). Indeed, a combination of the chemical versatility of iron and sulfur might be expected to generate ideal devices for accepting, donating, shifting, and storing electrons. Although we will not expand on the electron transfer function, we note one recent and spectacular illustration of this function implied by the x-ray structure of the [NiFe]-hydrogenase of *D. gigas* (*33*). Three clusters are aligned nearly linearly in the order $Fe_4S_4|Fe_3S_4|Fe_4S_4$ from the Ni–Fe active site at which the reaction $H_2 \rightarrow 2H^+ + 2e^-$ is catalyzed (Fig. 3). This juxtaposition of the four metal-containing sites in the enzyme would appear to prescribe the pathway for electron exit to the natural acceptor.

Other functions not of an oxidoreductive nature have emerged. These include the binding and activation of substrates at the unique iron site of **5b** in the catalytic function of aconitase (*34*) and related enzymes (*35*), and apparently stabilizing radicals in reactions occurring by a free-radical pathway (*36*). There is evidence that the clusters can function in coupling electron transfer to proton transport (*37*). In the "Rieske" proteins containing the cluster $[Fe_2S_2(S\cdot Cys)_2(N\cdot His)_2]$, ionization of a co-

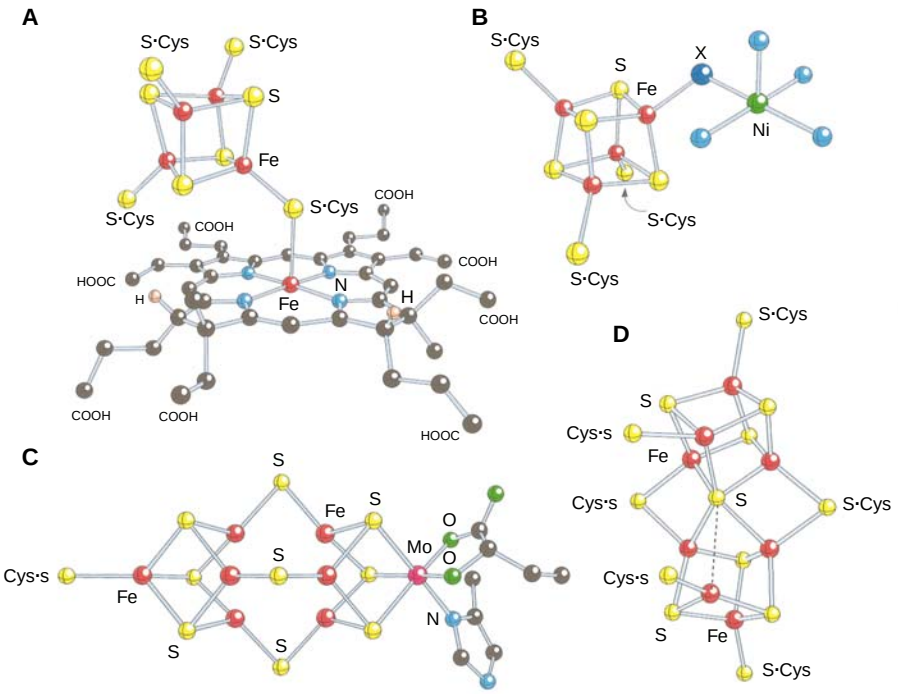

Fig. 2. Schematic structures of native assemblies in which a cubane-type or cuboidal iron-sulfur cluster is bridged to the other component of the active site: (**A**) *Escherichia coli* sulfite reductase (*11*); (**B**) carbon monoxide dehydrogenase (bridge moiety X is unidentified, and the ligands and stereochemistry at the Ni sites are not fully defined); (**C**) cofactor cluster of nitrogenase (*10*); and (**D**) P cluster of nitrogenase (*11*). Structures (A), (C), and (D) have been determined by crystallography; (B) has been deduced from spectroscopic evidence (*12*).

ordinated imidazole group may be coupled to oxidation-reduction (*38*). By binding Cys ligands from different subunits, iron-sulfur clusters effect dimer formation, as in the Fe protein of nitrogenase (*39*) and cluster F_x of Photosystem I (*40*). Further, by straddling protein structural elements, iron-sulfur clusters are able to stabilize structures that are required for specific functions. That appears to be the case with endonuclease III of *E. coli*, where a specific DNA binding site is stabilized (*41*). In a related function, clusters have been shown to protect proteins from the attack of intracellular proteases, as with an amidotransferase of *Bacillus subtilis* (*42*). Enzyme stability requires the presence of one Fe_4S_4 cluster. When this enzyme is exposed to dioxygen in vivo, the rates of inactivation and protein degradation are the same. The inactivation step is the destructive reaction of dioxygen with the cluster. Iron-sulfur clusters may also serve as storage devices for iron and possibly sulfide (*43*).

Even more intriguing are the findings that iron-sulfur clusters serve as sensors of iron, dioxygen, superoxide ion (O_2^-), and possibly nitric oxide (*44*–*48*). There appear to be (at least) two modes of sensing. In one, the oxidation $[Fe_2S_2]^{1+} \rightarrow [Fe_2S_2]^{2+}$ by dioxygen provides the signal for activation of a defense mechanism against superoxide, as observed with the SoxR protein of *E. coli* (*47*, *48*). In an alternative mechanism, oxidative disassembly or reassembly of a cluster provides the controlling signal, as in the FNR protein of *E. coli*. Here, the active FNR dimer dissociates into inactive monomers when the clusters are destroyed (*27*).

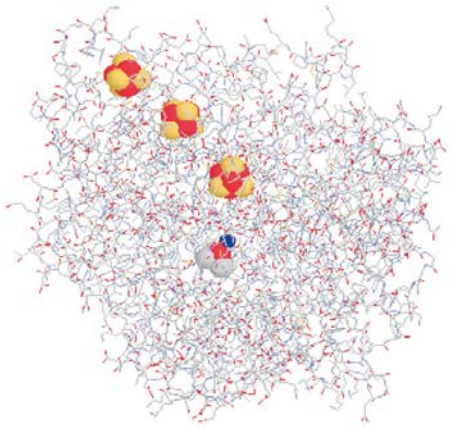

Fig. 3. Spatial disposition of the four metal centers in *D. gigas* hydrogenase (*33*). In terms of nearest distances between cysteinate sulfur ligands, the nickel-iron catalytic site (red and blue) is separated by 6.1 Å from the proximal Fe_4S_4 cluster. This unit is 5.7 Å from an Fe_3S_4 cluster, which is separated by 5.1 Å from the distal Fe_4S_4 cluster. The three-cluster array is an attractive electron transfer pathway, but the involvement of (all) clusters in transferring electrons to the probable physiological acceptor, cytochrome c_3, is currently uncertain.

A second case where cluster assembly and disassembly provide the signals is found with IRP-1, the iron regulatory protein (*44*, *45*). The control of intracellular iron levels depends critically on the function of two proteins: the transferrin receptor, which recognizes the iron-loaded transport protein transferrin and ushers it into cells, and the storage protein ferritin, which provides for reversible and safe storage of excess iron. The concentration of these proteins is regulated at the translational level by a single ingenious control system. The messenger RNAs (mRNAs) for transferrin receptor and for ferritin contain so-called iron-responsive elements (IREs). These are RNA stem-loop structures that occur in the untranslated regions. In the case of ferritin mRNA, one IRE is in the 5′ region, and in the transferrin receptor mRNA, five IREs are in the 3′ region. These IREs bind with high affinity to the iron regulatory protein (IRP). This ~100-kD protein is found in all higher forms of life from mollusks to insects and vertebrates. Iron regulatory protein is always present in an active or inactive form. It is activated during an iron deficiency and is inactivated when iron available for complexation is plentiful. When the IRE is in the 5′ region of the mRNA, as in ferritin mRNA, translation is blocked by the bound IRP. In transferrin receptor mRNA, however, five IREs are in the 3′ untranslated region and protect the mRNA from nucleolytic degradation when IRP is bound to at least three of them. Thus, IRP is able to adjust the levels of transferrin receptor and ferritin in an opposing sense, as required either for acquisition of iron for use or for storage of excess.

It was no minor surprise when it was discovered that the inactive form of IRP is identical to the cytoplasmic isoform of a long-known enzyme, the iron-sulfur protein aconitase, and that active IRP is apo-aconitase, lacking its $[Fe_4S_4]^{2+}$ cluster (*34*, *44*, *45*, *49*). When iron is scarce, the apo-form (the IRP) prevails, blocking ferritin synthesis and protecting transferrin receptor mRNAs. When iron becomes available again, holo-aconitase is reconstituted from IRP so that the protein loses its function as IRP, but can now be recognized by its aconitase activity. Thus, assembly and disassembly of the iron-sulfur cluster is the regulatory step (*46*), although it seems likely that some adjuvants, proteins, or small molecules are involved in the process. The IREs that bind IRP are present not only in ferritin and transferrin receptor mRNAs; they are also found in the mRNA for erythroid levulinic acid synthase, mitochondrial aconitase, and the iron subunit of succinate dehydrogenase (in *Drosophila*). Thus, there is cross talk between various regulatory pathways and metabolic systems (*45*).

Both the FNR and IRP systems provide challenging opportunities for studying iron-sulfur cluster assembly and disassembly in biological systems. Concerning the sensitivity of the sensors, we have established that the Fe_4S_4 cluster in wild-type FNR is extremely sensitive to dioxygen. However, a single amino acid mutation stabilizes the cluster by at least 100-fold in rate of decay (*26*). This single observation makes obvious that nature has a means to design, when required, sensors of greatly different sensitivities. Lastly, there are other proteins where an iron-sulfur cluster is indispensable to biological activity, but where its actual role has yet to be defined. Mammalian ferrochelatase (*50*), which inserts iron in protoporphryin during heme biosynthesis, is one such case. The enzyme is strongly inhibited by nitric oxide which destroys its Fe_2S_2 cluster, suggesting a possible role as an NO sensor. Another example is the DNA mismatch-repair protein MutY of *E. coli* (*51*), which seems to function in a way similar to endonuclease III.

Magnetochemistry

In the characterization of any paramagnetic metal site in biology, elucidation of electronic structure is imperative because it affects reactivity. Although it could not have been appreciated in the early phase of cluster synthesis and identification in proteins, iron-sulfur clusters pose uniquely challenging problems in molecular magnetism. Spectroscopic studies of iron-sulfur clusters have provided insight into cluster-mediated catalysis and electron transfer. Moreover, these studies have led to substantial advances in magnetochemistry, in particular to the appreciation of the phenomenon of spin-dependent delocalization (SDD, also called "double exchange"), which arises in delocalized mixed-valence systems. It is this aspect of iron-sulfur cluster research that we consider here. Experimentally, the effects of SDD are perhaps best illustrated by comparing the Mössbauer spectra of various clusters.

The isomer shift δ of a ^{57}Fe Mössbauer spectrum measures the *s*-electron density at the iron nucleus. Because the radial distributions of *d* and *s* electrons overlap, δ provides also a measure of the *d* electron population and is a good indicator of the oxidation state of iron sites (*52*). Experimentally, δ is obtained from the centroid of the Mössbauer spectrum and is quoted relative to a standard (such as iron metal) as a Doppler shift in velocity units (1 mm/s =

4.8×10^{-8} eV for ^{57}Fe). For instance, the high-spin FeS_4 sites of Fe^{3+} and Fe^{2+} rubredoxin (**1**) have $\delta \approx 0.25$ mm/s and $\delta \approx 0.70$ mm/s, respectively. Oxidized Fe_2S_2 clusters (**3**) contain two Fe^{3+} sites, each having $\delta \approx 0.27$ mm/s. A typical Mössbauer spectrum of a (reduced) $[Fe_2S_2]^{1+}$ cluster (Fig. 4A) exhibits two distinct quadrupole doublets with $\delta = 0.30$ mm/s (the inner doublet) and $\delta = 0.72$ mm/s, showing that the cluster contains a valence-localized Fe^{3+} site and a valence-localized Fe^{2+} site (Robin-Day class II mixed valence compound) (*53*). The ground state of the cluster has electronic spin $S = 1/2$ and exhibits the distinctive $g = 1.94$ electronic paramagnetic resonance (EPR) signal. The observation of *g* values less than 2.0 puzzled researchers for many years before it was shown that the ground-state properties result from antiferromagnetic coupling of high-spin Fe^{2+} ($S_a = 2$) and high-spin Fe^{3+} ($S_b = 5/2$) ions (*54*); this coupling is described by the Heisenberg–Dirac–van Vleck (HDvV) Hamiltonian $H = JS_a \cdot S_b$, in which *J* is the exchange coupling constant.

The Mössbauer spectra of $[Fe_3S_4]^{1+}$ clusters (**6**) exhibit one quadrupole doublet (Fig. 4B) with $\delta = 0.27$ mm/s, indicating three equivalent high-spin Fe^{3+} sites. Reduction of the cluster by one electron yields a state with cluster spin $S = 2$ that exhibits, for all $[Fe_3S_4]^0$ clusters studied to date, a pattern such as that observed for ferredoxin II isolated from *D. gigas* (*55*). The spectrum shown in Fig. 4C consists of two doublets with intensity ratio 1:2. The minor doublet has $\delta = 0.32$ mm/s and represents an Fe^{3+} site, whereas the major doublet belongs to two identical sites with $\delta = 0.46$ mm/s. The latter shift is about the mean of the δ values of a ferric and a ferrous FeS_4 site, indicating a delocalized $Fe^{2.5+}Fe^{2.5+}$ pair. Studies in strong applied magnetic fields have shown that the sites of the pair are indistinguishable even when magnetic and electric hyperfine parameters of the two sites are compared. Analysis of the ferredoxin II Mössbauer data led to the recognition that the presence of the delocalized $Fe^{2.5+}Fe^{2.5+}$ pair requires a treatment that takes SDD into account in addition to the commonly observed HDvV exchange (*55*). This analysis established that the $S = 2$ ground state of the $[Fe_3S_4]^0$ cluster can be viewed as arising from antiferromagnetic coupling of the $S_3 = 5/2$ spin of the Fe^{3+} site to the $S_{12} = 9/2$ spin of the delocalized $Fe^{2.5+}Fe^{2.5+}$ pair.

Spin-dependent delocalization is a version of the theory of double exchange developed by Zener (*56*) and by Anderson and Hasegawa (*57*). The basic idea can be illustrated (Fig. 5) by considering an electron in an orbital delocalized over metal sites, a and b, of a symmetric $Fe^{2+}Fe^{3+}$ dimer. A delocalized $Fe^{2.5+}Fe^{2.5+}$ dimer can be viewed as an $Fe^{3+}Fe^{3+}$ dimer that contains an additional, delocalizable electron. The spins of the five *d* electrons that occupy each Fe^{3+} site are aligned parallel by strong intra-atomic exchange. As the delocalizable electron "visits" each metal site, its spin aligns antiparallel to the spin of the d^5 core because of the Pauli exclusion principle. Because delocalization between sites a and b originates from electrostatic interactions, the transfer occurs without spin flip, and the itinerant electron will thus promote parallel alignment of the core spins of the two metal sites. Anderson and Hasegawa have shown that resonance delocalization in a mixed-valence dimer leads to an energy splitting $\pm B(S + 1/2)$, where *S* is the spin of the dimer. For an $Fe^{2.5+}Fe^{2.5+}$ dimer, the coupling constant *B* can be written as $B = \beta/5$, where β is the transfer integral between the two orbitals on sites a and b that contain the delocalized electron; β is the homolog of the resonance integral in Hückel molecular orbital theory. The plus and minus signs correspond, respectively, to bonding and antibonding combinations of the two metal orbitals. A simplified representation of SDD is shown in Fig. 5; diagrams stressing intra-atomic exchange are displayed elsewhere (*58*, *59*).

The ideas of Anderson and Hasegawa were incorporated by Papaefthymiou *et al.* (*55*) into the framework of a spin Hamiltonian that allows one to analyze and correlate the data obtained from various tech-

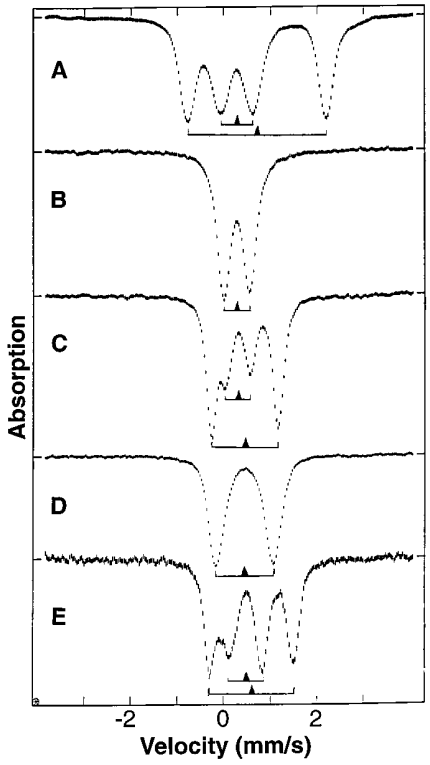

Fig. 4. Mössbauer spectra of iron-sulfur clusters. Quadrupole doublets are indicated by brackets, and isomer shifts are marked by triangles. (**A**) $[Fe_2S_2]^{1+}$ cluster of the Rieske protein from *Pseudomonas mendocina*, at temperature $T = 200$ K. (**B**) $[Fe_3S_4]^{1+}$ state of *D. gigas* ferredoxin II, $T = 90$ K. (**C**) $[Fe_3S_4]^0$ state of *D. gigas* ferredoxin II, $T = 15$ K. (**D**) $[Fe_4S_4]^{2+}$ cluster of *E. coli* FNR protein, $T = 4.2$ K. (**E**) $[Fe_4S_4]^{1+}$ cluster of *E. coli* sulfite reductase, $T = 110$ K.

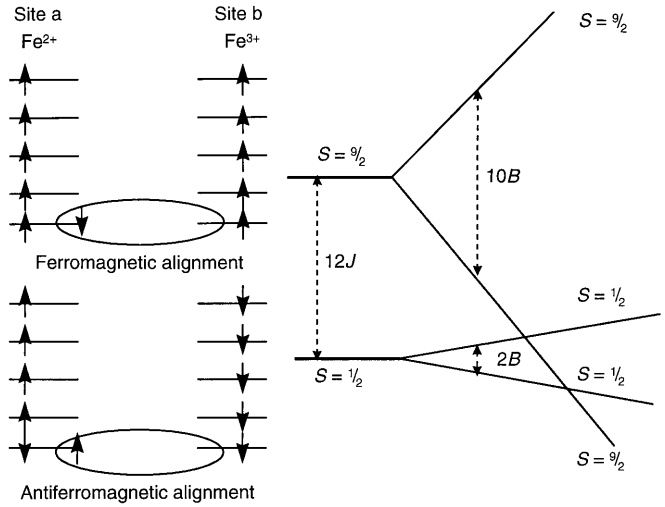

Fig. 5. Spin-dependent delocalization (SDD) for a symmetric $Fe^{2+}Fe^{3+}$ dimer, depicting ferromagnetic and antiferromagnetic spin alignments. Spin coupling of Fe^{2+} ($S_a = 2$) and Fe^{3+} ($S_b = 5/2$) by HDvV exchange leads to system states *S* with energies $JS(S + 1)/2$. On the right, the lowest ($S = 1/2$) and highest ($S = 9/2$) states of the resulting spin ladder are shown for $J > 0$. The sixth electron may be allocated to either site a or b; thus, each spin multiplet occurs twice. Resonance delocalization of the sixth electron (enclosed by the oval curve) mixes the degenerate $Fe^{2+}Fe^{3+}$ and $Fe^{3+}Fe^{2+}$ configurations, leading to an additional splitting $\pm B(S + 1/2)$. Delocalization is favored for the parallel spin alignment of the $S = 9/2$ state (top) but impeded for the $S = 1/2$ state. (As drawn for the antiferromagnetic configuration, the five remaining spins on site a do not represent a pure $S_a = 5/2$ spin state of an Fe^{3+} ion. Resonance interaction mixes only configurations with the same total spin. States with local spin $S_a < 5/2$ are unfavorable, leading to a reduction of the resonance splitting for the $S = 1/2$ state.) The diagram on the right shows that SDD may reverse the order of the spin states obtained from antiferromagnetic exchange.

niques. Noodleman and Baerends (*60*), and Noodleman, Case and co-workers (*58*) have treated the delocalization problem with broken-symmetry density functional theory. Girerd (*61*), Bominaar *et al.* (*62*), and Borshch *et al.* (*63*) have developed theoretical models that include vibronic interactions. The latter tend to localize electrons, and the situations encountered in real compounds reflect a delicate interplay between HDvV exchange, SDD, and vibronic trapping (*64*).

Figure 6 illustrates the localization-delocalization patterns of Fe/S clusters. Clusters of the Fe_4S_4 type (**5**) in their most common oxidation states contain delocalized $Fe^{2.5+}Fe^{2.5+}$ pairs. The presence of these pairs in Fe_4S_4 clusters was recognized as early as 1974 (*65*), and there is now general agreement that the cubane clusters, in their most common oxidation states (*66*), contain such pairs (Fig. 6E). Characteristic Mössbauer spectra of $[Fe_4S_4]^{2+}$ clusters (two equivalent $Fe^{2.5+}Fe^{2.5+}$ pairs with $\delta = 0.45$ mm/s) and the reduced $[Fe_4S_4]^{1+}$ state (one $Fe^{2.5+}Fe^{2.5+}$ pair with $\delta = 0.49$ mm/s and one $Fe^{2+}Fe^{2+}$ pair with $\delta = 0.62$ mm/s) are shown in Fig. 4, D and E, respectively. Clusters with $[Fe_2S_2]^{1+}$ cores generally show a localized pattern (Fig. 4A). The only exception is a cluster from a C*p* protein in which a Cys ligand has been mutated to a Ser; the cluster has an $S = 9/2$ ground state (*67*) that has been shown by Mössbauer spectroscopy to be valence-delocalized (*68*).

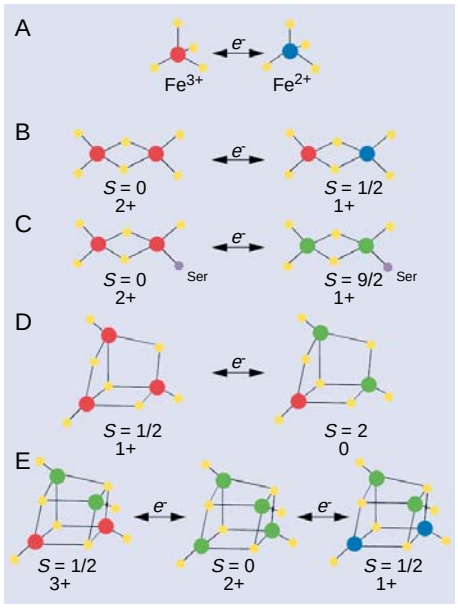

Fig. 6. Localization and delocalization patterns in Fe-S clusters, showing localized Fe^{3+} (red), localized Fe^{2+} (blue) sites and delocalized $Fe^{2.5+}Fe^{2.5+}$ pairs (green). Indicated also are the spin of the cluster and its core oxidation state. With one exception (row C), $[Fe_2S_2]^{1+}$ clusters have localized valences, as shown in row B. $[Fe_4S_4]^{1+}$ clusters most frequently have an $S = 1/2$ ground state; some protein-bound and synthetic clusters have $S = 3/2$ and exhibit a pattern of doublets reminiscent of a fully delocalized system.

The NMR solution studies of protein-bound Fe_4S_4 clusters have provided sequence-specific and stereospecific assignments of the β-CH_2 protons of cysteinate residues coordinated to the iron atoms of the cluster (*69*). If the proton coupling tensors are known (perhaps from electron nuclear double-resonance studies), one can determine the exchange coupling constants *B* and *J* from the temperature dependence of the hyperfine shifts of these protons. Moreover, the spin density at the iron atom to which a specific residue is bound can be determined, and thus, the distribution of spins within the cluster can be evaluated (*70*). The NMR studies of protein-bound $[Fe_4S_4]^{3+}$ clusters indicate that the delocalized pair can reside on different Fe_2S_2 faces of the cluster and that, on the NMR time scale (10^{-5} s), a cluster can exist in rapid equilibrium between the different forms (*69*).

The ^{57}Fe magnetic hyperfine tensors extracted from the Mössbauer spectra of $[Fe_3S_4]^0$ clusters provide strong evidence that the delocalized pair has spin $S = 9/2$ (*55*). For the delocalized pair of $[Fe_4S_4]^{3+}$ clusters, the situation is more varied. These clusters have been studied with Mössbauer and EPR spectroscopy, with protein NMR, and with magnetic susceptibility (*70, 71*). The $[Fe_4S_4]^{3+}$ clusters have also been obtained by γ irradiation of synthetic $[Fe_4S_4]^{2+}$ complexes and investigated by ^{57}Fe and ^1H electron nuclear double-resonance spectroscopy (*72*). From these data, $S = 9/2$ (*71*), $S = 7/2$ (*72*), and $S = 9/2,7/2$ mixed spin (*73*) states have been inferred for the delocalized pair. The active site of oxidized sulfite reductase (Fig. 2A) contains a coupled siroheme-Fe_4S_4 assembly for which the siroheme iron is linked by a cysteinyl sulfur to one of the iron atoms of the cluster. This link provides an exchange pathway that perturbs the spin structure of the cluster. Considerable insight into the electronic structure of the $[Fe_4S_4]^{2+}$ cluster has been obtained from analysis of the perturbed state (*62*).

Reliable experimental values for the double-exchange parameter *B* are scarce for a variety of reasons, foremost of which is the problem of fitting data to models that contain many unknowns. For instance, the spin structure of $[Fe_4S_4]^{3+}$ clusters depends on as many as six values of *J* and at least one *B* parameter. In addition, parameters describing dynamic and static trapping mechanisms influence the energy level structure. Magnetic susceptibility data (*71*) of a synthetic $[Fe_4S_4]^{3+}$ cluster have been fitted with *B* values ranging from $\sim$10 cm^{-1} (*73*) to 600 cm^{-1} (*71*) [see also (*64*)]. The parameter *B* can be obtained from the splitting of the bonding and antibonding combinations of the local orbitals that contain the delocalized electron; optical transitions between these orbitals yield an intervalence band. Large values of *B*, $\sim$1000 cm^{-1}, have been inferred for $[Fe_2S_2]^{1+}$ clusters in plant-type ferredoxins (*74*). Most recently, low-temperature magnetic circular dichroism studies of $[Fe_2S_2]^{1+}$, $[Fe_3S_4]^0$, and $[Fe_4S_4]^{1+,3+}$ clusters by Johnson and co-workers (*75*) have led to the identification of intervalence bands in the near-infrared region of the magneto-optical spectra, indicating that $B \sim 800$ to 900 cm^{-1} for all three cluster types. These values agree well with those obtained from density functional calculations, which suggest *B* values of 700 to 900 cm^{-1} for Fe_4S_4 clusters (*58, 64*). It should be noted that valence localization as identified by Mössbauer spectroscopy in the $S = 1/2$ ground state of $[Fe_2S_2]^{1+}$ clusters does not exclude large values for *B*. When trapping mechanisms (Δ) dominate SDD, the *B* term appears in a second-order perturbation proportional to $B^2(S + 1/2)^2/\Delta \approx B^2S(S + 1)/\Delta$ (apart from a spin-independent constant) (*61*). This term has the same $S(S + 1)$ dependence as HDvV exchange and contributes, probably substantially, to the measured *J* values (*76*).

Finally, a theoretical analysis indicates that intramolecular electron delocalization and HDvV exchange can have an important impact on the rate constant for intermolecular electron transfer reactions involving exchange-coupled clusters (*77*). One should consider spin-state variability depending on cluster environment as a possible control factor for substrate specificity and gated electron transfer. Considering that electronic structure and electron transfer capabilities depend on an intricate interplay of HDvV exchange, SDD, and vibronic trapping, we are perhaps just beginning to appreciate why nature has found so many uses for Fe-S clusters.

REFERENCES AND NOTES

1. D. I. Arnon, F. R. Whatley, M. B. Allen, *Nature* **180**, 182 (1957); *ibid.*, p. 1325; A. San Pietro and H. M. Lang, *J. Biol. Chem.* **231**, 261 (1958).
2. L. E. Mortenson, R. C. Valentine, J. E. Carnahan, *Biochem. Biophys. Res. Commun.* **7**, 448 (1962).
3. H. Beinert and R. H. Sands, *ibid.* **3**, 41 (1960).
4. W. Lovenberg, Ed., *Iron-Sulfur Proteins* (Academic Press, New York, 1973), vols. I and II.
5. T. G. Spiro, Ed., *Iron-Sulfur Proteins* (Wiley-Interscience, New York, 1982); R. Cammack, *Adv. Inorg. Chem.* **38**, 281 (1992).
6. J. M. Berg and R. H. Holm, in *Iron-Sulfur Proteins*, T. G. Spiro, Ed. (Wiley-Interscience, New York, 1982), pp. 1–66.

7. R. H. Holm, P. Kennepohl, E. I. Solomon, *Chem. Rev.* **96**, 2239 (1996).
8. R. H. Holm, *Acc. Chem. Res.* **16**, 2565 (1977); K. S. Hagen, J. G. Reynolds, R. H. Holm, *J. Am. Chem. Soc.* **103**, 4054 (1981).
9. J. Zhou, Z. Hu, E. Münck, R. H. Holm, *J. Am. Chem. Soc.* **118**, 1966 (1996).
10. M. K. Chan, J. Kim, D. C. Rees, *Science* **260**, 792 (1993); J. W. Peters *et al*., *Biochemistry* **36**, 1181 (1997).
11. J. A. Christner *et al.*, *J. Am. Chem. Soc.* **106**, 6786 (1984); B. R. Crane, L. M. Siegel, E. D. Getzoff, *Science* **270**, 59 (1995).
12. S. W. Ragsdale and M. Kumar, *Chem. Rev.* **96**, 2515 (1996); Z. Hu *et al.*, *J. Am. Chem. Soc.* **118**, 830 (1996).
13. W. O. Gillum, L. E. Mortenson, J.-S. Chen, R. H. Holm, *J. Am. Chem. Soc.* **99**, 584 (1977); W. H. Orme-Johnson and R. H. Holm, *Methods Enzymol.* **53**, 268 (1978).
14. J. J. G. Moura *et al.*, *J. Biol. Chem.* **257**, 6259 (1982).
15. T. A. Kent *et al.*, *Proc. Natl. Acad. Sci. U.S.A.* **79**, 1096 (1982).
16. T. A. Kent *et al.*, *J. Biol. Chem.* **260**, 6871 (1985).
17. M.-P. Golinelli, L. A. Akin, B. R. Crouse, M. K. Johnson, J. Meyer, *Biochemistry* **35**, 8995 (1996).
18. M. C. Kennedy *et al.*, *J. Biol. Chem.* **259**, 14463 (1984).
19. K. S. Hagen, A. D. Watson, R. H. Holm, *J. Am. Chem. Soc.* **105**, 3905 (1983).
20. I. Moura, J. J. G. Moura, E. Münck, V. Papaefthymiou, J. LeGall, *ibid.* **108**, 349 (1986); M. G. Finnegan *et al.*, *Inorg. Chem.* **34**, 5358 (1995).
21. J. N. Butt *et al.*, *J. Am. Chem. Soc.* **113**, 6663 (1991).
22. J. Zhou *et al.*, *ibid.* **114**, 10843 (1992); J. Zhou, J. W. Raebiger, C. A. Crawford, R. H. Holm, *ibid.* **119**, 6242 (1997).
23. D. Coucouvanis, *Acc. Chem. Res.* **24**, 1 (1991); K. D. Demadis, S. M. Malinak, D. Coucouvanis, *Inorg. Chem.* **35**, 4038 (1996).
24. G. L. Anderson and J. B. Howard, *Biochemistry* **23**, 2118 (1984).
25. M. J. Ryle, W. N. Lanzilotta, L. C. Seefeldt, R. C. Scarrow, G. M. Jensen, *J. Biol. Chem.* **271**, 1551 (1996).
26. N. Khoroshilova, C. Popescu, E. Münck, H. Beinert, P. J. Kiley, *Proc. Natl. Acad. Sci. U.S.A.* **94**, 6087 (1997).
27. N. Khoroshilova, H. Beinert, P. J. Kiley, *ibid.* **92**, 2499 (1995); B. A. Lazazzera, H. Beinert, N. Khoroshilova, M. C. Kennedy, P. J. Kiley, *J. Biol. Chem.* **271**, 2762 (1996).
28. A. Martin *et al.*, *Proc. Natl. Acad. Sci. U.S.A.* **87**, 598 (1990); B. Shen *et al.*, *ibid.* **92**, 10064 (1995).
29. M. C. Kennedy, M. H. Emptage, H. Beinert, *J. Biol. Chem.* **259**, 3145 (1984).
30. J. G. Reynolds and R. H. Holm, *Inorg. Chem.* **20**, 1873 (1981).
31. M. J. Carney, G. C. Papaefthymiou, R. B. Frankel, R. H. Holm, *ibid.* **28**, 1497 (1989)
32. M. K. Johnson, in *Encyclopedia of Inorganic Chemistry*, R. B. King, Ed. (Wiley, New York, 1994), pp. 1896–1915.
33. A. Volbeda *et al.*, *Nature* **373**, 580 (1995); A. Volbeda *et al.*, *J. Am. Chem. Soc.* **118**, 12989 (1996).
34. H. Beinert, M. C. Kennedy, C. D. Stout, *Chem. Rev.* **96**, 2335 (1996).
35. D. H. Flint and R. M. Allen, *ibid.*, p. 2315.
36. C. R. Staples *et al.*, *Biochemistry* **35**, 11425 (1996).
37. J. L. C. Duff, J. L. J. Breton, J. N. Butt, F. A. Armstrong, A. J. Thomson, *J. Am. Chem. Soc.* **118**, 8593 (1996).
38. T. Iwasaki, T. Imai, A. Urushiyama, T. Oshima, *J. Biol. Chem.* **271**, 27659 (1996).
39. J. B. Howard and D. C. Rees, *Chem. Rev.* **96**, 2965 (1996).
40. J. H. Golbeck and D. A. Bryant, *Curr. Top. Bioenerg.* **16**, 83 (1991).
41. M. M. Thayer, H. Ahern, D. Xing, R. P. Cunningham, J. A. Tainer, *EMBO J.* **14**, 4108 (1995).
42. J. A. Grandoni, R. L. Switzer, C. A. Makaroff, H. Zalkin, *J. Biol. Chem.* **264**, 6058 (1989).
43. R. K. Thauer and P. Schönheit, in *Iron-Sulfur Proteins*; T. G. Spiro, Ed. (Wiley-Interscience, New York, 1982), pp. 329–341.
44. T. A. Rouault *et al.*, *BioMetals* **5**, 131 (1992).
45. W. Hentze and L. C. Kühn, *Proc. Natl. Acad. Sci. U.S.A.* **93**, 8175 (1996).
46. H. Beinert and P. Kiley, *FEBS Lett.* **382**, 218 (1996).
47. P. Gaudu and B. Weiss, *Proc. Natl. Acad. Sci. U.S.A.* **93**, 10094 (1996).
48. E. Hidalgo, J. M. Bollinger Jr., T. M. Bradley, C. T. Walsh, B. Demple, *J. Biol. Chem.* **270**, 20908 (1995).
49. D. J. Haile *et al.*, *Proc. Natl. Acad. Sci. U.S.A.* **89**, 11735 (1992).
50. H. A. Dailey, M. G. Finnegan, M. K. Johnson, *Biochemistry* **33**, 403 (1994); V. M. Sellers, M. K. Johnson, H. A. Dailey, *ibid.* **35**, 2699 (1996).
51. M. L. Michaels, L. Pham, Y. Nghiem, C. Cruz, J. H. Miller, *Nucleic Acids Res.* **18**, 3841 (1990).
52. P. Gütlich, R. Link, A. Trautwein, *Mössbauer Spectroscopy and Transition Metal Chemistry* (Springer Verlag, Berlin, 1978).
53. M. B. Robin and P. Day, *Adv. Inorg. Chem. Radiochem.* **10**, 247 (1967).
54. R. H. Sands and W. R. Dunham, *Q. Rev. Biophys.* **7**, 443 (1975).
55. V. Papaefthymiou, J.-J. Girerd, I. Moura, J. J. G. Moura, E. Münck, *J. Am. Chem. Soc.* **109**, 4703 (1987).
56. C. Zener, *Phys. Rev.* **82**, 403 (1951).
57. P. W. Anderson and H. Hasegawa, *ibid.* **100**, 675 (1955).
58. L. Noodleman, C. Y. Peng, D. A. Case, J.-M. Mouesca, *Coord. Chem. Rev.* **144**, 199 (1995).
59. B. Lamotte and J.-M. Mouesca, *C. R. Acad. Sci. Paris Ser. IIB* **324**, 117 (1997).
60. L. Noodleman and J. Baerends, *J. Am. Chem. Soc.* **106**, 2316 (1984).
61. J.-J. Girerd, *J. Chem. Phys.* **79**, 1766 (1983).
62. E. L. Bominaar, Z. Hu, E. Münck, J.-J. Girerd, S. A. Borshch, *J. Am. Chem. Soc.* **117**, 6976 (1995).
63. S. A. Borshch, E. L. Bominaar, G. Blondin, J.-J. Girerd, *ibid.* **115**, 5155 (1993).
64. For further commentary on electron delocalization in mixed-valence iron-sulfur clusters, see the collected papers in *J. Biol. Inorg. Chem.* **1**, 173–188 (1996).
65. D. P. E. Dickson *et al.*, *J. Phys. (Paris)* **35**, C6–343 (1974).
66. Recent Mössbauer and EPR studies of the fully reduced Fe protein of nitrogenase have demonstrated an all-ferrous $[Fe_4S_4]^0$ cluster with an $S = 4$ ground state. All iron sites of the $[Fe_4S_4]^0$ cluster have $\delta =$ 0.68 mm/s. H. Angove, S. J. Yoo, B. K. Burgess, E. Münck, *J. Am. Chem. Soc*., in press.
67. B. R. Crouse, J. Meyer, M. K. Johnson, *ibid.* **117**, 9612 (1995).
68. C. Achim, M.-P. Golinelli, E. L. Bominaar, J. Meyer, E. Münck, *ibid.* **118**, 8168 (1996).
69. L. Banci *et al.*, *Biochemistry* **32**, 9387 (1993).
70. I. Bertini, S. Ciurli, C. Luchinat, *Struct. Bonding (Berlin)* **83**, 1 (1995).
71. J. Jordanov, E. K. H. Roth, P. H. Fries, L. Noodleman, *Inorg. Chem.* **29**, 4288 (1990).
72. The following single-crystal studies show that the delocalized pair can reside on different faces of the cube: J.-M. Mouesca, G. Rius, B. Lamotte, *J. Am. Chem. Soc*. **115**, 4714 (1993); J. Gloux, P. Gloux, B. Lamotte, J.-M. Mouesca, G. Rius, *ibid.* **116**, 1953 (1994).
73. M. Belinskiy, I. Bertini, O. Galas, C. Luchinat, *Inorg. Chim. Acta* **243**, 91 (1996).
74. D. A. Gamelin, E. L. Bominaar, M. L. Kirk, K. Wieghardt, E. I. Solomon, *J. Am. Chem. Soc.* **118**, 8085 (1996).
75. E. C. Duin *et al.*, in preparation.
76. O. Kahn, *Molecular Magnetism* (VCH, New York, 1993), chap. 13.
77. E. L. Bominaar, C. Achim, S. A. Borshch, J.-J. Girerd, E. Münck, *Inorg. Chem.*, in press.

78. Research in iron-sulfur cluster chemistry and biochemistry has been supported by NIH grants GM 12394, GM 34812, and 5-K06 GM 18442 (H.B.), GM 28856 (R.H.H.), and GM 22701 (E.M.), and by NSF grant MCB 94–06225 (E.M.).